Supplemental data

Elevated CXCL1 expression in gp130-deficient endothelial cells impairs neutrophil migration in mice

Longbiao Yao, Tadayuki Yago, Bojing Shao, Zhenghui Liu, Robert Silasi-Mansat, Hendra Setiadi, Florea Lupu, and Rodger P. McEver

Supplemental methods

Mice

All mouse protocols were approved by the Institutional Animal Care and Use Committee of the Oklahoma Medical Research Foundation. Mice lacking gp130 in both hematopoietic and endothelial cells (termed EHCgp130$^{-/-}$ mice in this paper) were made by crossing *gp130*$^{flox/flox}$ mice with transgenic mice expressing Cre recombinase under control of a *Tie2* promoter/enhancer to generate *gp130*$^{flox/flox}$/*Tcre*$^{+}$ mice[1]. Control mice were *gp130*$^{flox/flox}$ mice that do not express Cre (*gp130*$^{flox/flox}$/*Tcre*$^{-}$) or *gp130*$^{+/+}$/*Tcre*$^{+}$ mice. Both groups of control mice exhibited the same phenotype and are referred to as WT mice. Radiation chimeric mice lacking gp130 in hematopoietic or endothelial cells were generated as described previously[1]. Mice lacking gp130 in myeloid cells (MCgp130$^{-/-}$ mice) were generated by crossing *gp130*$^{flox/flox}$ mice with mice expressing Cre under the control of the lysozyme M promoter[2]. Control mice were *gp130*$^{flox/flox}$ mice that do not express Cre (*gp130*$^{flox/flox}$/*LysMcre*$^{-}$) or *gp130*$^{+/+}$/*LysMcre*$^{+}$ mice. Both groups of control mice exhibited the same phenotype and are referred to as WT mice. LysM-GFP^{+} mice[3] were crossed with EHCgp130$^{-/-}$ mice to generate EHCgp130$^{-/-}$/LysM-GFP^{+}

mice. All strains were fully backcrossed into the C57BL/6J background.

Cells

Murine endothelial cells from lung and murine leukocytes from bone marrow were isolated as described[1]. Murine neutrophils were isolated as described[4]. Briefly, bone marrow leukocytes were isolated by flushing femurs and tibias with HBSS. Red blood cells were lysed with 150 mM NH_4Cl, 10 mM $NaHCO_3$, 1 mM EDTA for 20 seconds. The cells were washed twice with HBSS, and then resuspended in 3 ml of 45% Percoll (GE Healthcare) solution in 150 mM NaCl. The cells were loaded on top of a Percoll density gradient prepared by layering 81, 62, 55, and 50% Percoll solution. After centrifugation at 1,200 g for 30 minutes, the cell band between the 81 and 62% layer was harvested, washed twice, and resuspended in HBSS containing Ca^{2+} and Mg^{2+} and 0.1% BSA. Murine splenocytes were isolated by straining spleens in HBSS without Ca^{2+} or Mg^{2+} plus 0.5% human serum albumin through 40-μm mesh. The cell suspension was centrifuged at 100 x g for 5 minutes. Red blood cells in the pellet were lysed with 150 mM NH_4Cl, 10 mM $NaHCO_3$, 1 mM EDTA for 20 seconds. The pellet was resuspended in 5 ml HBSS without Ca^{2+} or Mg^{2+} plus 0.5% human serum albumin and centrifuged again at 100 x g for 5 minutes. The pellet was resuspended at 2 x 10^6 cells/ml in the same buffer.

Reagents

Rat anti-murine P-selectin mAb RB40.34[5] was a gift from Dietmar Vestweber (Max Planck Institute of Biomolecular Medicine, Muenster, Germany). Rat anti-murine E-selectin mAb 9A9[6] was a gift from Barry Wolitzky (Immune Tolerance Network, San Francisco, CA). Rat anti-β_2 integrin mAb GAME46, rat anti-CD31 mAb, hamster anti-ICAM-1 mAb 3E2, FITC-conjugated rat anti-β_2 integrin mAb, PE-conjugated rat anti-L-selectin mAb, PE-conjugated rat

anti-PSGL-1 mAb, and PE-conjugated rat anti-CXCR2 mAb were from BD Biosciences. Rat anti-CXCL1 mAb, rat anti-CXCR2 mAb, and murine recombinant CXCL1, TNF-α, VCAM-1 IgG, and ICAM-1 IgG were from R&D Systems. Rabbit anti-CXCL1 was from PeproTech. Murine recombinant CXCL2, and Alexa 546-conjugated streptavidin were from BioLegend. Rabbit anti-neutrophil elastase antibody was from Dako. Alexa 568-conjugated donkey anti-rabbit IgG and Alexa 488-conjugated donkey anti-rat IgG were from Invitrogen. FITC-conjugated goat anti-rabbit IgG and Cy 3-conjugated goat anti-rat IgG were from Jackson ImmunoResearch.

Intravital microscopy

Intravital microscopy of the cremaster muscle of anesthetized mice was performed as described[7-9]. Mice were anesthetized with an intraperitoneal injection of 1.25% Avertin (tribromoethanol/amylene hydrate, 0.2 ml/10g body weight). Exteriorization of the cremaster muscle was completed within 10 minutes (trauma-induced inflammation). In some mice, 10 μg anti-P-selectin mAb, anti-β_2 integrin mAb, anti-CXCL1 mAb, or anti-CXCR2 mAb was injected intravenously 10 minutes before cremaster muscle exteriorization. For TNF-α-induced inflammation, mice were injected intrascrotally with 500 ng murine TNF-α 2 hours before cremaster muscle exteriorization. In some mice, 4 μg pertussis toxin (PTx; Sigma) was injected intravenously 2 hours before cremaster muscle exteriorization or 5 minutes before TNF-α injection. Leukocyte rolling, adhesion, and migration were recorded in 3 to 5 venules from each mouse. In other experiments, bone marrow leukocytes from WT or EHCgp130$^{-/-}$ mice were labeled with red fluorescent dye (PKH26, Sigma). The labeled cells were resuspended in HBSS at 10^8/ml and injected (200 μl per mouse) intravenously into WT or EHCgp130$^{-/-}$ mice. Rolling and adhesion of labeled cells was observed by fluorescent microscopy using a Nikon eclipse

microscope (E600FN) with a Nikon mercury lamp and 510-560-nm excitation filter. In some experiments, recombinant murine CXCL1 or synthetic peptide WKYMVm (Millipore)[10] in HBSS was superfused over the cremaster muscle immediately after exteriorization. After 30 minutes (and after 60 and 90 minutes in some experiments), leukocyte emigration was measured as the number of extravascular leukocytes per microscopic field of view (x20 objective lens) adjacent to the selected postcapillary venules[11,12]. Intraluminal crawling of neutrophils (each followed at 3 frames/s for at least 5 minutes) was measured as described previously[12,13]. In some experiments, 1 U heparinase III (Sigma-Aldrich), or 10 μg or 100 μg anti-CXCL1 mAb in 200 μl HBSS was injected intravenously 30 minutes before cremaster muscle exteriorization. Hemodynamic parameters, measured as described[8], were comparable in all experimental groups.

Leukocyte adhesion in dermal venules of the ear was measured as described[9,14], except that GFP-labeled leukocytes in EHCgp130$^{-/-}$/LysM-GFP^{+} mice or control LysM-GFP^{+} mice were visualized.

In some experiments, Fluoresbrite Red microspheres (0.5 μm diameter, Polysciences, Inc.) were coated with control or anti-CXCL1 mAb. 10^{10} microspheres in 100 μl saline were injected through the retro-orbital venous plexus. After 20 minutes, the mice were sacrificed and the cremaster muscle was rapidly fixed (no trauma). Alternatively, the cremaster muscle was exteriorized (trauma) before sacrificing the mice and fixing the tissue. Fluorescent microspheres within venules were observed with a Nikon eclipse microscope (E600FN) at x40 magnification (Nikon Fluo 40 x, numerical aperature:1.2 water immersion) with a Nikon mercury lamp and 510-560-nm excitation filter and quantified by Elements software (Nikon).

Bone marrow transplantation

Bone marrow transplantation was performed as described[1]. Flow cytometry with mAbs to CD45 isoforms to distinguish donor and recipient hematopoietic cells confirmed >95% reconstitution with donor cells six weeks after transplantation.

Confocal microscopy

Frozen tissue sections were fixed in acetone at -20°C for 10 minutes. The sections were incubated with rat anti-CD144 (VE-Cadherin) mAb followed by Alexa 568-conjugated donkey anti-rat IgG. The stained specimens were mounted in Vectashield hard-set (Vector) on a slide in a chamber. Images were visualized on a Zeiss Axiovert 200M (Carl Zeiss, LLC) microscope at x63 magnification (Plan-Apochromat 100 x, numerical aperture: 1.4 oil), and captured by a Carl Zeiss AxioCam MRm Rev. 3.0 camera. The acquisition software was Carl Zeiss AxioVision Ver. 4.8.

For whole-mount confocal imaging of unstimulated cremaster muscle, LysM-GFP^{+} or EHCgp130$^{-/-}$/LysM-GFP^{+} mice, both expressing GFP in myeloid cells, were injected intravenously with biotin-conjugated rat anti-CD31 mAb and then sacrificed. The cremaster muscle was then rapidly isolated and fixed in situ with 4% paraformaldehyde in PBS for 30 minutes. For whole-mount confocal imaging of skin, histamine (Sigma, 10 µg in 50 µl saline) or 50 µl saline was injected intradermally into the shaved dorsal skin of LysM-GFP^{+} or EHCgp130$^{-/-}$/LysM-GFP^{+} mice. After 20 minutes, mice were injected with biotin-conjugated rat anti-CD31 mAb and sacrificed after 10 minutes (30 minutes after the initial histamine or saline injection). Skin was then rapidly excised and fixed with 4% paraformaldehyde in PBS for 30 minutes. Some mice were injected with 20 µg anti-P-selectin mAb intravenously 30 minutes before the intradermal injections. The fixed cremaster muscle or skin fragments were permeabilized with 0.1% saponin in PBS for 30 minutes and then placed in blocking buffer (PBS-saponin and 1%

BSA) for 1 hour. The specimens were stained with secondary Alexa 546-conjugated streptavidin. In some experiments, fixed frozen tissue sections were incubated with rabbit anti-gp130 or with rabbit anti-CXCL1 polyclonal antibody and rat anti-CD31 mAb followed by Alexa 568-conjugated donkey anti-rabbit IgG and Alexa 488-conjugated donkey anti-rat IgG. Confocal microscopy was conducted with a Nikon C1 inverted confocal microscope on a Nikon TE2000U microscope. The scanning was done at ×60 magnification (Nikon CFI plan Apo 60.0 × 1.20 water immersion lens) by using Argon 488, HeNe 546 and HeNe 634 lasers as excitation light sources. The acquisition software was EZ-C1 version 3.6 (Nikon). Image collection parameters (neutral density filters, pinhole, and detector gains) were kept constant during image acquisition to make reliable comparisons between specimens. Image acquisition was done sequentially for each fluorescence channel to avoid bleed through. Pixel fluorescence intensity was estimated using EZ-C1 (Nikon) or ImageJ (NIH) software.

For whole-mount confocal imaging and 3D rendering of trauma- or TNF-α-stimulated cremaster muscle, the tissue was fixed in situ with 4% paraformaldehyde in PBS for 30 minutes, dissected and immersed again in the same fixative for 60 minutes, and then washed three times with PBS. The fixed cremaster muscle fragments were permeabilized with 0.01% saponin and 0.1% Triton X-100 in PBS for 30 minutes, treated with blocking buffer (PBS-saponin and 1% BSA) for 1 h, incubated with rabbit anti-neutrophil elastase antibody and rat anti-murine CD31 antibody overnight at 4˚C, and then washed three times with PBS. The specimens were incubated with secondary anti-rabbit and anti-rat antibodies conjugated with FITC and Cy3, respectively and then with To-Pro3 (Invitrogen) to counterstain cell nuclei. The stained specimens were mounted in Vectashield hard-set (Vector) on a slide in a chamber to avoid damaging the tissue. Confocal microscopy was conducted with a Nikon C1 inverted confocal microscope. The

scanning was done at ×60 magnification (Nikon CFI plan Apo 60.0 × 1.20 water immersion lens) by using Argon 488, HeNe 546 and HeNe 634 lasers as excitation light sources. Optical sections were taken at 0.5-μm intervals. The wavelength settings of the acquisition detectors were adjusted to minimize crossover between the emission wavelengths of each fluorophore, and scanning was conducted in a sequential mode to further minimize crossover. 3D reconstruction of the confocal image stacks and background subtraction were accomplished by using IMARIS V. 6.4 software (Bitplane, Zurich, Switzerland). The IMARIS Surpass module was used to generate 3D reconstructions of cremaster muscle microvasculature.

Electron microscopy

Cremaster muscle was fixed in situ with a mixture of 3% paraformaldehyde and 2% glutaraldehyde in 0.1 M sodium cacodylate buffer for 15 minutes before dissection. Tissue samples were further fixed by immersion in the same fixative for 1 hour, followed by 1% tannic acid (30 minutes) and postfixation in 1% osmium tetroxide (1 hour). The samples were subsequently dehydrated in a graded ethanol series and embedded in epoxy resin (EMS). Ultrathin sections (80 nm) were obtained using an ultramicrotome (RMC 7000, RMC) equipped with a diamond knife. Sections were stained with uranyl acetate and lead citrate before being viewed with a Hitachi H-7600 electron microscope equipped with a 4 megapixel digital monochrome camera and AMT-EM image acquisition software (Advanced Microscopy Techniques).

Real-time RT-PCR and ELISA

Total RNA from cultured murine lung endothelial cells was prepared using the RNeasy RNA extraction kit (Qiagen) with DNase I treatment following the manufacturer's instructions. Murine cremaster muscle was dissected and homogenized in QIAzol lysis buffer (Qiagen), and

total RNA was isolated using the RNeasy RNA Mini kit (Qiagen) following the manufacturer's instructions. To generate cDNA, total RNA (100 ng) from each of triplicate samples was converted into cDNA using random primers and Superscript III reverse transcriptase (Invitrogen). Primers for amplifying cDNA (supplemental Table 3) were designed and synthesized by Integrated DNA Technologies. The cDNA samples were subjected to real-time PCR amplification using an ABI Prism 7900HT Sequence Detection System (Applied Biosystems) and a QuantiTect SYBR Green PCR kit (Qiagen). The level of target gene expression was normalized against the actin expression in each sample, and the level of target mRNA was expressed as relative fold changes (fold change = $2^{-\Delta\Delta CT}$, where $\Delta\Delta CT = (C_{T,\ target} - C_{T,\ actin})_{Time\ x} - (C_{T,\ target} - C_{T,\ actin})_{Time\ 0}$.

Proteins were extracted from homogenized murine cremaster muscle using Tissue-PE LB buffer (G-Biosciences). Protein concentration was measured with the Micro BCA Protein Assay Kit (Thermo Scientific). ELISA for CXCL1 in serum or tissue extract was measured with the DuoSet mouse KC ELISA Kit (R&D Systems).

Immunoblots

Lung endothelial cells isolated from WT or EHCgp130$^{-/-}$ mice were lysed in 50 mM NaCl, 50 mM Tris-HCl (pH 7.5), 1% Triton-X, 50 mM NaF, 1 mM PMSF, 10 μg/ml aprotinin, 5 μg/ml leupeptin, 1 mM Na_3VO_4 and 5 mM EDTA. Proteins were resolved by SDS-PAGE, transferred to Immobilon P (Millipore) membranes, and probed with primary antibodies, followed by HRP-conjugated goat anti-rat IgG (Thermo Scientific), using a chemiluminescence detection system (GE Healthcare).

Flow cytometry

Heparinized blood from WT or EHCgp130$^{-/-}$ mice was obtained by cardiac puncture. Red blood cells were lysed by adding 150 mM NH_4Cl, 10 mM $NaHCO_3$, 1 mM EDTA. After lysis, leukocytes were washed with PBS and centrifuged at 100 x g for 10 minutes at room temperature. The pellet was resuspended in HBSS without Ca^{2+} or Mg^{2+} containing 0.5% human serum albumin. Some cells were incubated with 100 μg/ml CXCL1 at 37˚C for 30 minutes. After washing with HBSS without Ca^{2+} or Mg^{2+} containing 0.5% human serum albumin, leukocytes were pretreated with 20 μg/ml anti-murine CD16/CD32 Fc receptor blocking mAb (BD Biosciences) for 10 minutes at 4˚C, and stained with FITC-conjugated anti-murine β_2 integrin, PE-conjugated anti-murine L-selectin, PE-conjugated anti-murine PSGL-1, or PE-conjugated anti-murine CXCR2 mAb for 20 minutes. The cells were analyzed on a FACScaliber using CellQuest software. Neutrophils were identified based on scatter properties and high expression of Gr-1[7].

Chemokine binding to endothelial cells

Murine CXCL2 was labeled with FITC using the SureLINK Fluorescence Labeling Kit (KPL) following the manufacturer's protocol. Chemokine binding to lung endothelial cells was performed as described previously[15], with slight modifications. Briefly, murine lung endothelial cells were pretreated with PBS containing 100 μg/ml heparin for 10 minutes at room temperature and washed three times with PBS. Some cells were further pretreated with 1 U/ml heparinase III for 30 minutes at 37˚C and washed. The cells were then incubated with 2 μg/ml FITC-conjugated CXCL2 for 30 minutes at 4˚C, washed, and analyzed by flow cytometry.

Chemokine transport across endothelial cells

Chemokine transport across cultured endothelial cells was performed as described previously[15], with slight modifications. Murine lung endothelial cells were seeded on

fibronectin-coated transwells of 6.5-mm diameter with 0.4-μm pore filters (BD Biosciences). After 7 days, confluent monolayers had formed. The endothelial cells were treated with DMEM containing 1% BSA plus 100 μg/ml heparin for 10 minutes at room temperature and then washed with DMEM containing 1% BSA. Some cells were further pretreated with 1 U/ml heparinase III in the same buffer for 30 minutes and washed. Then, 0.1 ml DMEM containing 1% BSA was added to the upper compartment and 0.6 ml DMEM containing 1% BSA plus 2 μg/ml FITC-conjugated CXCL2 was added to the lower compartment. After incubating 30 minutes at 37˚C, the buffer in the upper chamber was removed and replaced with 0.1 ml DMEM containing 1% BSA plus 100 μg/ml heparin to release bound FITC-conjugated CXCL2. After 30 minutes at 37˚C, this buffer was pooled with the original upper-chamber buffer. The fluorescence intensity of the pooled buffer was measured in a FLUOstar Omega microplate reader (BMG Labtech).

Flow chamber assay

Leukocyte adhesion under flow was measured as described previously[7]. Bone marrow leukocytes from WT or EHCgp130$^{-/-}$ mice (10^6/ml in HBSS containing Ca^{2+} and Mg^{2+} plus 0.5% human serum albumin) were perfused over TNF-α-stimulated (25 ng/ml, 4 h) monolayers of lung endothelial cells from WT or EHCgp130$^{-/-}$ mice in dishes mounted in a parallel-plate flow chamber at 1.0 dyne/cm^2. In some experiments, stimulated endothelial cell monolayers were preincubated with 20 μg/ml anti-P-selectin mAb, anti-E-selectin mAb, anti-ICAM-1 mAb, or anti-CXCL1 mAb, or isotype-matched control mAb. In other experiments, leukocytes were preincubated with 20 μg/ml anti-CXCR2 mAb or isotype-matched control mAb. In some experiments, WT splenocytes (2 x 10^6/ml in HBSS containing Ca^{2+} and Mg^{2+} plus 0.5% human serum albumin) were perfused at 0.5 dyne/cm^2 over immobilized murine control IgG or murine VCAM-1 IgG in the presence or absence of rat control mAb or rat anti-murine VCAM-1 mAb

M/K-1[8]. After 5 minutes, cells were analyzed using a videomicroscopy system coupled to a digital analysis system.

Transendothelial migration assay

Migration assays were performed in transwells of 6.5-mm diameter with 5-μm pore filter membranes coated with fibronectin (BD Biosciences). Murine lung endothelial cells were plated at 25,000 cells per filter. The confluent endothelial cells were pretreated with 25 ng/ml TNF-α for 4 hours and then washed three times with DMEM containing 1% BSA. In some experiments, 5-μm pore filter membranes were coated with 20 μg/ml murine ICAM-1 IgG with or without the indicated concentration of recombinant murine CXCL1. Bone marrow neutrophils or bone marrow leukocytes (10^5 cells in 0.1 ml DMEM containing 1% BSA) were added to the upper compartment, and 0.6 ml DMEM containing 1% BSA with or without 100 μM WKYMVm or the indicated concentration of recombinant murine CXCL1 was added to the lower compartment. In some experiments, recombinant murine CXCL1 at the indicated concentration was added to DMEM in the upper compartment. Assays were conducted in a humidified 37°C chamber in 5% CO_2 for 60 minutes. After removing the filter inserts, 50,000 beads (15-μm diameter, Polybead polystyrene microspheres, Polysciences) in 0.1 ml PBS were added to each well. Flow cytometry was used to quantify the ratio of migrated neutrophils to beads by their respective scatter properties[16,17].

Thioglycollate-induced peritonitis

The number of neutrophils entering the peritoneum 4 hours after injection of thioglycollate was measured as described previously[7].

Blood vessel permeability assay

The modified Miles assay for histamine-stimulated vascular permeability was performed as described previously[18]. Briefly, 100 µl of 1% Evan's blue dye (Sigma) in PBS was injected intravenously. After 10 minutes, histamine (Sigma, 10 µg in 50 µl saline) or 50 µl saline was injected intradermally into the shaved dorsal skin. After 30 minutes, the skin was excised and extracted with formamide for 5 d. The extracted dye was measured at 620 nm. Some mice were injected with 20 µg anti-P-selectin mAb intravenously 30 minutes before the intradermal injections.

References

1. Yao L, Yokota T, Xia L, Kincade PW, McEver RP. Bone marrow dysfunction in mice lacking the cytokine receptor gp130 in endothelial cells. *Blood*. 2005;106:4093-4101.

2. Clausen BE, Burkhardt C, Reith W, Renkawitz R, Forster I. Conditional gene targeting in macrophages and granulocytes using LysMcre mice. *Transgenic Res*. 1999;8(4):265-277.

3. Faust N, Varas F, Kelly LM, Heck S, Graf T. Insertion of enhanced green fluorescent protein into the lysozyme gene creates mice with green fluorescent granulocytes and macrophages. *Blood*. 2000;96(2):719-726.

4. Lowell CA, Fumagalli L, Berton G. Deficiency of Src family kinases p59/61hck and p58c-fgr results in defective adhesion-dependent neutrophil functions. *J Cell Biol*. 1996;133(4):895-910.

5. Ley K, Bullard DC, Arbonés ML, et al. Sequential contribution of L- and P-selectin to leukocyte rolling in vivo. *J Exp Med*. 1995;181:669-675.

6. Labow MA, Norton CR, Rumberger JM, et al. Characterization of E-selectin-deficient mice: demonstration of overlapping function of the endothelial selectins. *Immunity*. 1994;1:709-720.

7. Yago T, Shao B, Miner JJ, et al. E-selectin engages PSGL-1 and CD44 through a common signaling pathway to induce integrin $\alpha_L\beta_2$-mediated slow leukocyte rolling. *Blood*. 2010;116:485-494.

8. Xia L, Sperandio M, Yago T, et al. P-selectin glycoprotein ligand-1-deficient mice have impaired leukocyte tethering to E-selectin under flow. *J Clin Invest*. 2002;109:939-950.

9. Liu Z, Miner JJ, Yago T, et al. Differential regulation of human and murine P-selectin expression and function in vivo. *J Exp Med*. 2010;207:2975-2987.

10. Christophe T, Karlsson A, Dugave C, Rabiet MJ, Boulay F, Dahlgren C. The synthetic peptide Trp-Lys-Tyr-Met-Val-Met-NH2 specifically activates neutrophils through FPRL1/lipoxin A4 receptors and is an agonist for the orphan monocyte-expressed chemoattractant receptor FPRL2. *J Biol Chem*. 2001;276(24):21585-21593.

11. Massena S, Christoffersson G, Hjertstrom E, et al. A chemotactic gradient sequestered on endothelial heparan sulfate induces directional intraluminal crawling of neutrophils. *Blood*. 2010;116(11):1924-1931.

12. Heit B, Liu L, Colarusso P, Puri KD, Kubes P. PI3K accelerates, but is not required for, neutrophil chemotaxis to fMLP. *J Cell Sci*. 2008;121(Pt 2):205-214.

13. Phillipson M, Heit B, Colarusso P, Liu L, Ballantyne CM, Kubes P. Intraluminal crawling of neutrophils to emigration sites: a molecularly distinct process from adhesion in the recruitment cascade. *J Exp Med*. 2006;203(12):2569-2575.

14. Weninger W, Ulfman LH, Cheng G, et al. Specialized contributions by α(1,3)-fucosyltransferase-IV and FucT-VII during leukocyte rolling in dermal microvessels. *Immunity*. 2000;12(6. 6):665-676.

15. Wang L, Fuster M, Sriramarao P, Esko JD. Endothelial heparan sulfate deficiency impairs L-selectin- and chemokine-mediated neutrophil trafficking during inflammatory responses. *Nat Immunol*. 2005;6(9):902-910.

16. Zabel BA, Nakae S, Zuniga L, et al. Mast cell-expressed orphan receptor CCRL2 binds chemerin and is required for optimal induction of IgE-mediated passive cutaneous anaphylaxis. *J Exp Med*. 2008;205(10):2207-2220.

17. Frommhold D, Ludwig A, Bixel MG, et al. Sialyltransferase ST3Gal-IV controls CXCR2-mediated firm leukocyte arrest during inflammation. *J Exp Med*. 2008;205(6):1435-1446.

18. Wegmann F, Petri B, Khandoga AG, et al. ESAM supports neutrophil extravasation, activation of Rho, and VEGF-induced vascular permeability. *J Exp Med*. 2006;203(7):1671-1677.

Supplemental table 1

Peripheral blood counts

	WBC ($x\ 10^3/\mu L$)	NE ($x\ 10^3/\mu L$)	LY ($x\ 10^3/\mu L$)	MO ($x\ 10^3/\mu L$)	RBC ($x\ 10^6/\mu L$)	Hgb (g/dL)	PLT ($x\ 10^3/\mu L$)
WT (n = 25)	4.5 ± 0.3	1.2 ± 0.2	3.1 ± 0.2	0.1 ± 0.05	9.0 ± 0.2	12 ± 1.0	1000 ± 100
EHCgp130$^{-/-}$ (n = 30)	11.0 ± 0.5	6.0 ± 1.2	4.5 ± 0.4	0.3 ± 0.05	8.9 ± 0.5	10 ± 1.5	1200 ± 200

WBC, total leukocytes; NE, neutrophils; LY, lymphocytes, MO, monocytes, RBC, red blood cells; Hgb, hemoglobin; PLT, platelets

Supplemental table 2

Hemodynamic and microvascular parameters

	Anti-P-sel	Anti-β2	PTx	Anti-CXCL1	Anti-CXCR2	Heparinase III	Mice (n)	Venules (n)	Diameter (μm)	Centerline velocity (μm/s)
WT	-	-	-	-	-	-	8	20	34 ± 3	2200 ± 100
	+	-	-	-	-	-	5	12	34 ± 5	2000 ± 100
	-	+	-	-	-	-	4	12	32 ± 4	2400 ± 200
	-	-	+	-	-	-	5	13	29 ± 3	2300 ± 150
	-	-	-	+	-	-	4	12	30 ± 3	2200 ± 200
	-	-	-	-	+	-	5	11	35 ± 6	1900 ± 150
$gp130^{-/-}$	-	-	-	-	-	-	4	12	33 ± 3	2000 ± 200
	+	-	-	-	-	-	4	14	30 ± 2	2200 ± 150
	-	+	-	-	-	-	4	13	33 ± 4	2400 ± 200
	-	-	+	-	-	-	4	12	34 ± 4	2000 ± 150
	-	-	-	+	-	-	4	12	32 ± 5	2400 ± 100
	-	-	-	-	+	-	4	14	30 ± 3	2300 ± 100
	-	-	-	-	-	+	4	12	33 ± 4	2000 ± 200

Supplemental table 3

Sequences of primers used for real-time quantitative RT-PCR

Gene	Sense primer	Antisense primer
CXCL1	5'-CGAAGTCATAGCCACACTCAA-3'	5'-GAGCAGTCTGTCTTCTTTCTCC-3'
CXCL2	5'-GACAGAAGTCATAGCCACTCTC-3'	5'-GCCTTGCCTTTGTTCAGTATC-3'
ICAM-2	5'-CTGGAGCCTGTCTCTTCTTATC-3'	5'-GTGGCTTCTACTATCTGCTTCTC-3'
JAM-A	5'-GTCCTGGTAACACTGATTCTCC-3'	5'-TACTGGGCTGGCTGTAAATG-3'
JAM-C	5'-GGGAGTCCTTGTTGTCCTTATT-3'	5'-CCTGGGCTCTTATAGCTTTCTC-3'
ESAM	5'-CCCATCCTGATCTGGTTCTTG-3'	5'-CAGGGCTGTTCCAGGTTTAT-3'
CD99	5'-GTGATGTCACTACTGCCAAAGA-3'	5'-CTCCTTGTGAGTGGAGGTTATG-3'
CD99L2	5'-ATCCAGCTACATCTCCTACCA-3'	5'-ACAACAGCTTCCAGGTTCTC-3'
PECAM-1	5'-TGGACACTACACCTGCAAAG-3'	5'-ACGACTGGAGGAGAACTCTAA-3'
VCAM-1	5'-GAGGGAGACACCGTCATTATC-3'	5'-CGAGCCATCCACAGACTTTA-3'
ICAM-1	5'-GTGATGGCAGCCTCTTATGT-3'	5'-GGGCTTGTCCCTTGAGTTT-3'
β-Actin	5'-ACCAGTTCGCCATGGATGAC-3'	5'-TGCCGGAGCCGTTGTC-3'

Supplemental figure legends

Supplemental Figure 1. **Endothelial cell gp130 is efficiently deleted in skin and cremaster muscle of EHCgp130$^{-/-}$ mice.** Frozen tissue sections were incubated with rabbit anti-gp130 antibody and rat anti-CD31 mAb followed by Alexa 568-conjugated donkey anti-rabbit IgG and Alexa 488-conjugated donkey anti-rat IgG. Nuclei were stained with DAPI (blue). Note near complete loss of gp130 staining (red) in CD31-positive endothelial cells (green) of EHCgp130$^{-/-}$ tissues. Bar, 20 μm. The data are representatiave of three experiments.

Supplemental Figure 2. **Peripheral blood neutrophils from WT and EHC gp130-/- mice express equivalent levels of major glycoproteins.** Peripheral blood leukocytes from WT or EHCgp130$^{-/-}$ mice were incubated without CXCL1 (resting) or with CXCL1 (activated) for 30 minutes at 37˚C. The indicated surface molecule was then analyzed by flow cytometry. Neutrophils were defined by scatter properties and high expression of Gr-1. The data are representative of three independent experiments.

Supplemental Figure 3. **Injecting anti-β_2 integrin mAb does not detach already arrested neutrophils in trauma-stimulated venules of EHCgp130$^{-/-}$ mice.** Neutrophil firm adhesion in trauma-stimulated venules of cremaster muscle from WT or EHCgp130$^{-/-}$ mice was measured before and after injecting anti-β_2 integrin mAb intravenously. The data represent the mean ± SEM from 15 to 20 venules from four to five mice in each group.

Supplemental Figure 4. **ICAM-1 but not VCAM-1 contributes to neutrophil firm adhesion in trauma-stimulated venules of EHCgp130$^{-/-}$ mice.** (A) Quantification of mRNA for ICAM-1 and VCAM-1 in cremaster muscle. (B) Neutrophil firm adhesion was measured in venules of cremaster muscle from WT or EHCgp130$^{-/-}$ mice subjected to surgical trauma. Before surgery some mice were injected intravenously with anti-ICAM-1 or anti-VCAM-1 mAb. (C) Adhesion of WT splenocytes to immobilized VCAM-1 IgG or control IgG under flow was measured in the presence or absence of anti-VCAM-1 mAb or isotype-control mAb. The data in A and C present the mean ± SEM from three independent experiments. The data in B represent the mean ± SEM from 15 to 20 venules from four to five mice in each group.

Supplemental Figure 5. **gp130-deficient endothelial cells bind and transport chemokine normally.** (A) Binding of CXCL2-FITC to cultured lung endothelial cells from WT or EHCgp130$^{-/-}$ mice was measured by flow cytometry. As indicated, some endothelial cells were pretreated with heparinase to degrade heparan-sulfate glycosaminoglycans. (B) Lung endothelial cells from WT or EHCgp130$^{-/-}$ mice were cultured on transwell membranes. As indicated, some endothelial cells were pretreated with heparinase to degrade heparan-sulfate glycosaminoglycans. DMEM containing 1% BSA was added to the upper compartment and DMEM containing 1% BSA plus CXCL2-FITC was added to the lower compartment. After incubating 30 min at 37˚C, the upper-chamber buffer was collected. The membrane was further incubated with DMEM plus heparin to remove bound CXCL2-FITC. After 30 minutes at 37˚C, this buffer was pooled with the original upper-chamber buffer. The fluorescence intensity of the pooled buffer, representing transport of CXCL2-FITC to the upper chamber, was measured. The

data in A are representative of three independent experiments. The data in B represent the mean ± SEM from three experiments.

Supplemental Figure 6. **Even prolonged supervision of CXCL1 or WKYMVm does not promote transendothelial migration of neutrophils in EHCgp130$^{-/-}$ mice.** CXCL1 (2 μg/ml) or WKYMVm peptide (100 μM) was superfused on trauma-stimulated cremaster muscle of EHCgp130$^{-/-}$ mice. After 30, 60, or 90 minutes, the number of emigrated extravascular leukocytes was measured. The data represent the mean ± SEM from 15 to 20 venules from four to five mice.

Supplemental Figure 7. **Intraluminal crawling of neutrophils is markedly reduced in venules of EHCgp130$^{-/-}$ mice.** CXCL1 was superfused on trauma-stimulated cremaster muscle of WT or EHCgp130$^{-/-}$ mice. The mobility of adherent neutrophils in venules was monitored by video microscopy. (A) Percentage of adherent neutrophils that crawled. (B) The intraluminal crawling velocity was measured by dividing displacement by tracking time (at least 5 minutes) for each crawling cell. The data represent the mean ± SEM for at least 100 cells from 15 to 20 venules from four to five mice in each group.

Supplemental Figure 8. **Deletion of gp130 in endothelial cells does not alter expression of endothelial junction proteins.** (A) Quantification of mRNA for ICAM-2, JAM-A, JAM-C, ESAM, CD99, CD99L2, or PECAM-1 in unstimulated cremaster muscle from WT or EHCgp130$^{-/-}$ mice. (B) Frozen sections of cremaster muscle from WT or EHCgp130$^{-/-}$ mice were

stained with anti-VE-Cadherin mAb (red) and DAPI (blue). Bar, 10 μm. The data in A represent the mean ± SEM from three experiments. The data in B are representative of three experiments.

Supplemental Figure 9. **Anti-P-selectin and anti-E-selectin mAbs block neutrophil rolling and arrest, whereas anti-β_2 integrin mAb blocks only arrest on TNF-α-stimulated lung endothelial cells under flow.** Monolayers of cultured lung endothelial cells from WT or EHCgp130$^{-/-}$ mice were stimulated with TNF-α for 4 hours. The number of WT neutrophils rolling or firmly adherent (arrest) on each monolayers was measured. As indicated, endothelial cells were pretreated with anti-P-selectin and anti-E-selectin mAbs, or leukocytes were pretreated with anti-β_2 integrin mAb. The data represent the mean ± SEM from three experiments.

Supplemental Video 1. **Video recording of neutrophil intraluminal crawling in cremaster-muscle venules of a WT mouse in response to superfused CXCL1.** The original 2-minute image is played back 20 times faster. Most adherent neutrophils crawl in random directions.

Supplemental Video 2. **Video recording demonstrating lack of neutrophil intraluminal crawling in cremaster-muscle venules of a EHCgp130$^{-/-}$ mouse in response to superfused CXCL1.** The original 2-minute image is played back 20 times faster. Virtually all adherent neutrophils remain stationary.

Supplemental Figure 1

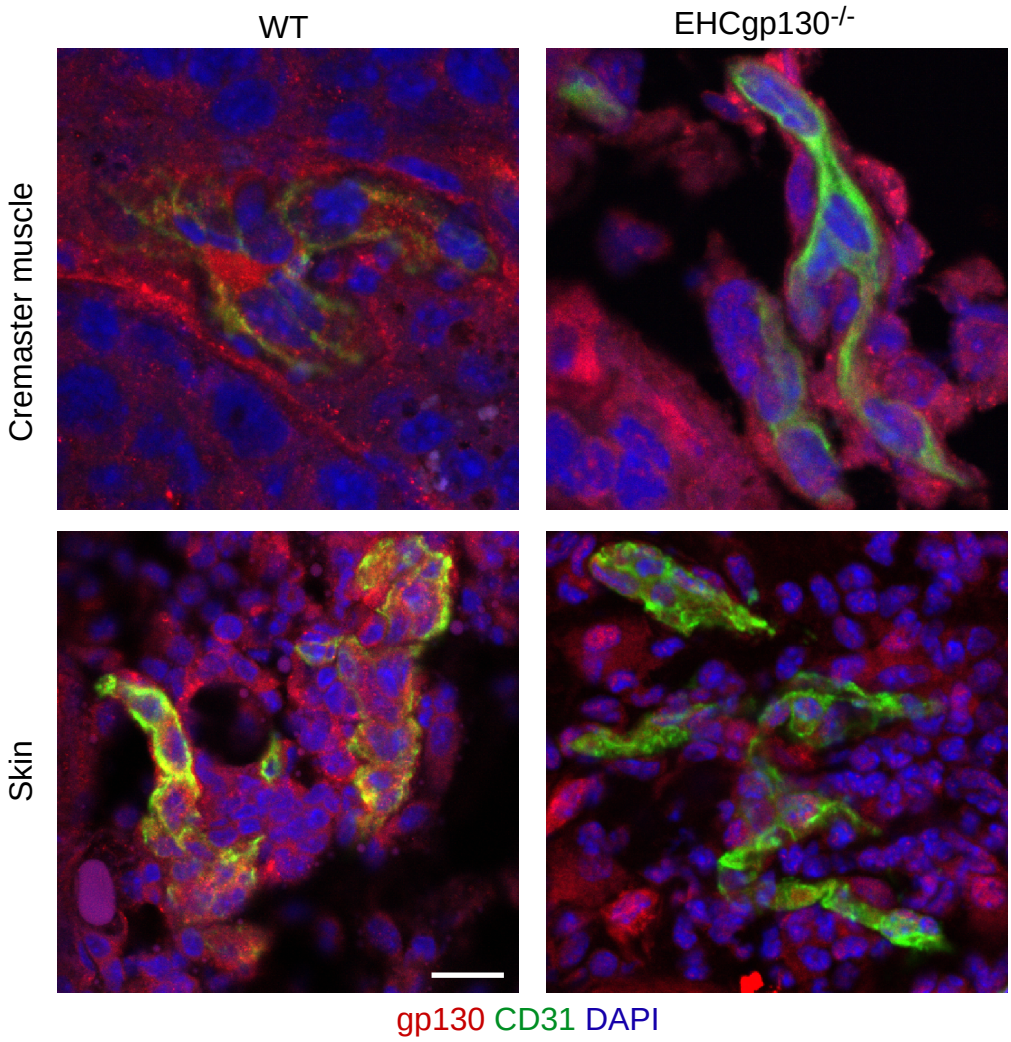

Supplemental Figure 2

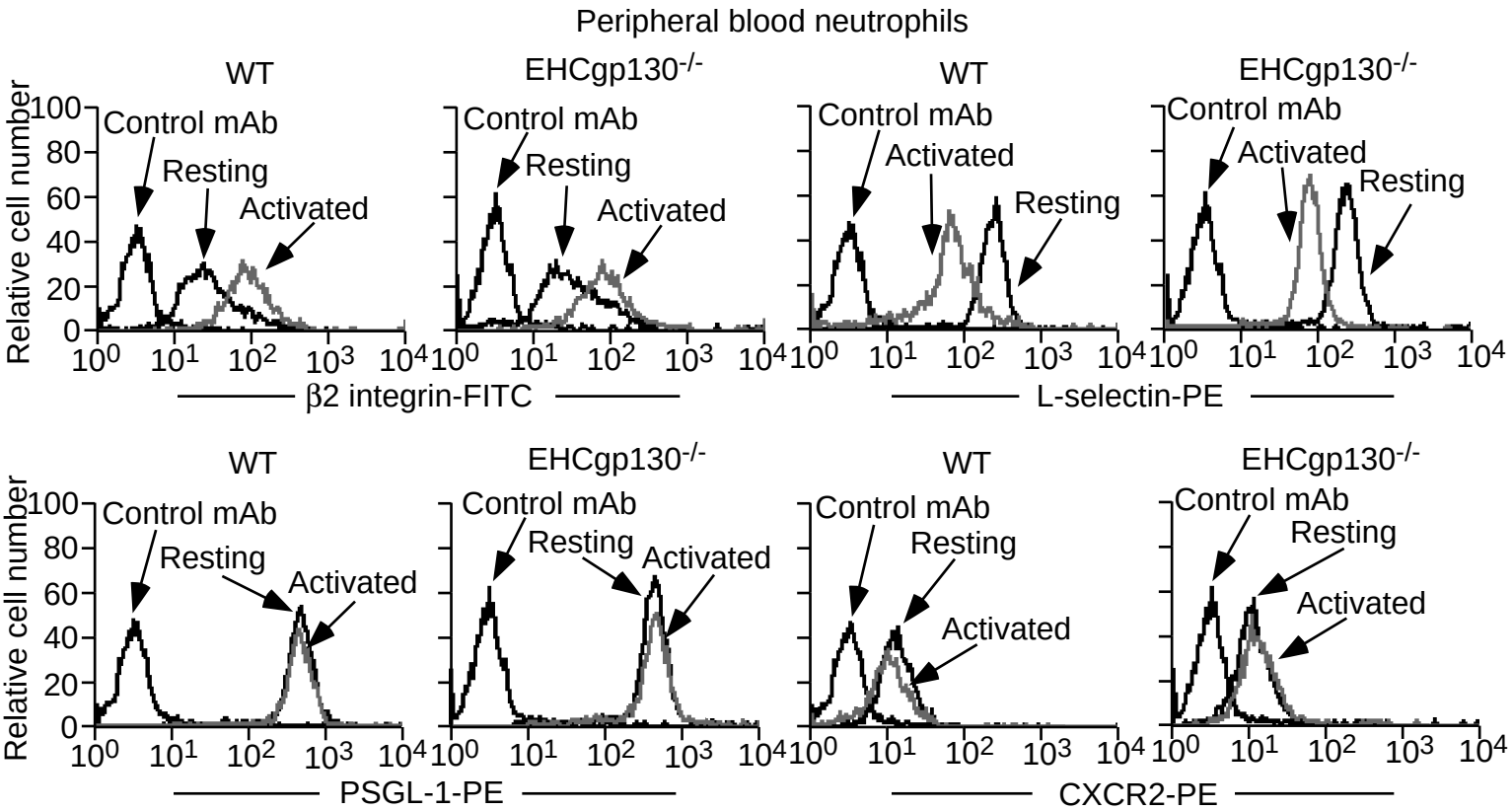

Supplemental Figure 3

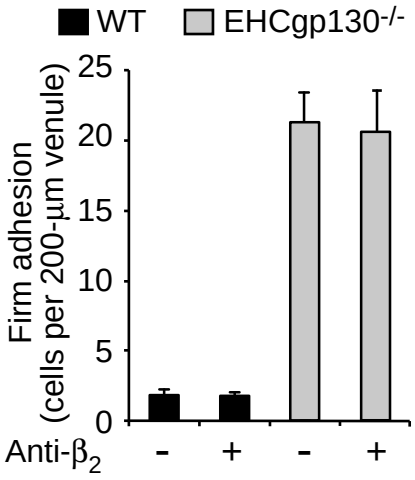

Supplemental Figure 4

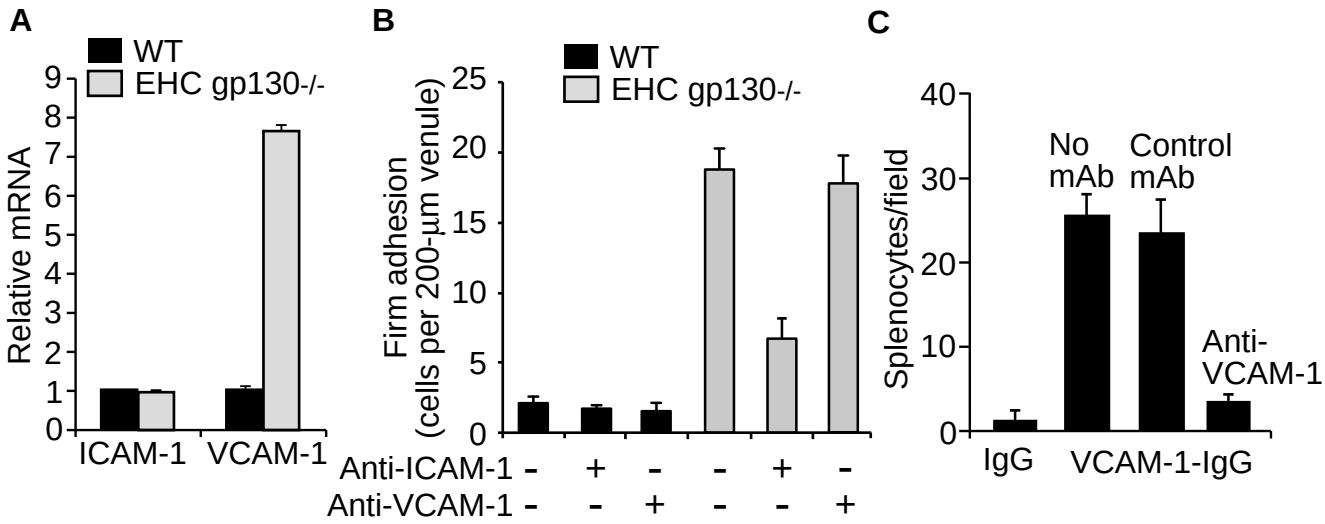

Supplemental Figure 5

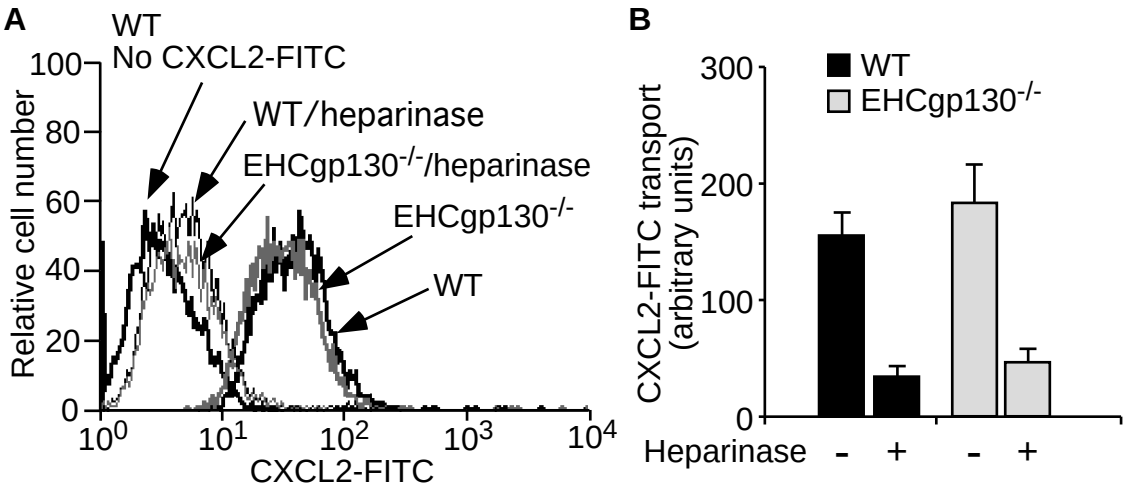

Supplemental Figure 6

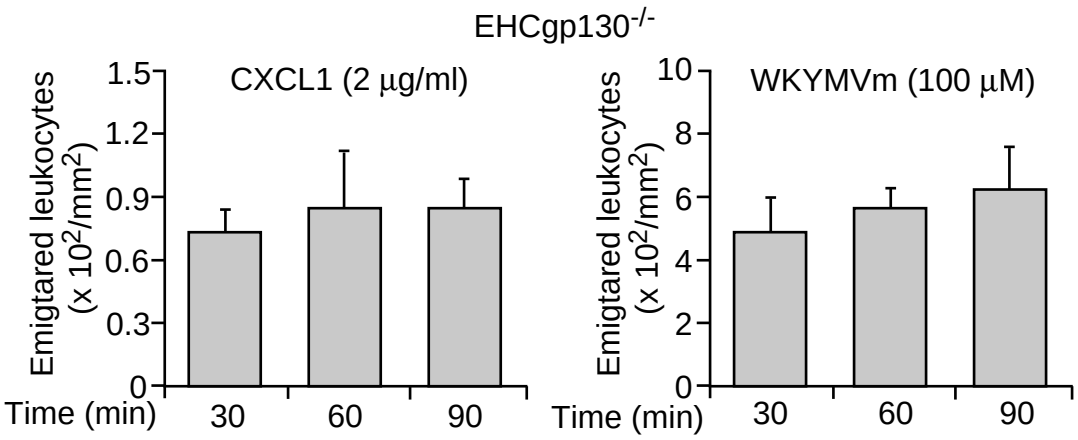

Supplemental Figure 7

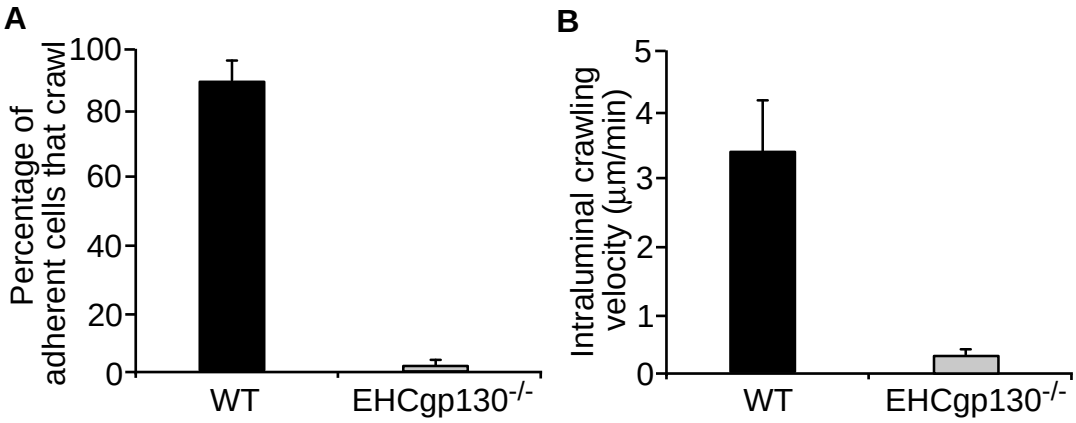

Supplemental Figure 8

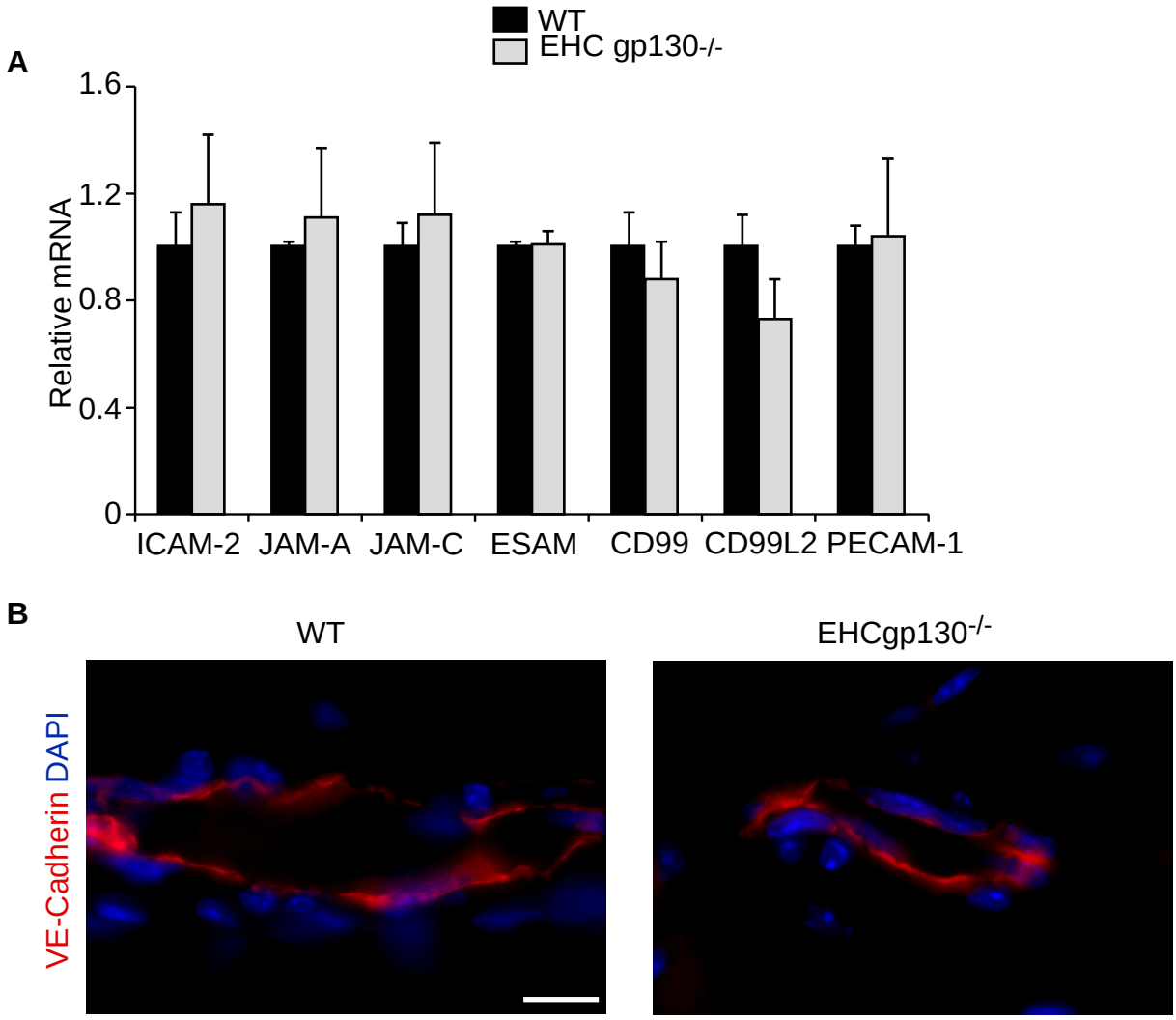

Supplemental Figure 9